

CHAPTER 89

LOADS ON SLOPING SEADYKES AND REVETMENTS FROM WAVE-INDUCED SHOCK PRESSURES

JOACHIM GRÜNE ¹

ABSTRACT

This paper deals with detailed studies on wave-induced pressures on sloping seadykes and revetments. The presented results are found as well from extensive field measurements at the coast of the German Bight as from full - scale laboratory tests in the LARGE WAVE CHANNEL (GWK) at Hannover, Germany. Summaring the results, a generalisation of shock pressure occurrence with respect to deterministic and stochastic characteristics and a "dynamic" loading model is presented.

INTRODUCTION

Shock pressures occuring on sloping dyke surfaces are damped more frequently compared to those on vertical walls. Furthermore, especially under real sea state conditions, partly they are mixed with pressure components from waves and wave run-ups. This results in a more complex analysis of shock pressures.

The author has demonstrated (GRÜNE, 1988a and 1988b), that for detailed statements on the loads from shock pressures an analysis of pressure-time histories from high-speed records is necessary instead of a simple peak value analysis. A scheme for the definition of shock pressure-time history parameters (anatomy parameters) was presented (Fig. 1) and its application was shown examplarily for compression domain with the pressure-time histories of individual breaking waves, measured in field. Furthermore first examples of some results from the anatomy parameter analysis have been presented. In this paper further results of the ongoing research work will be presented.

¹ Dipl.-Ing., senior researcher, deputy operation manager of the *Joint Institution LARGE WAVE CHANNEL (GWK) of the University Hannover and the Technical University Braunschweig*,
Grosser Wellenkanal, Merkurstrasse 11, 3000 Hannover, Germany

SHOCK PRESSURE ANALYSIS

As shown by GRÜNE (1988a and 1988b), the numberless different occurring shapes of pressure-time histories may be summarized by parameters (anatomy parameters) as defined in fig. 1, and divided into two domains:

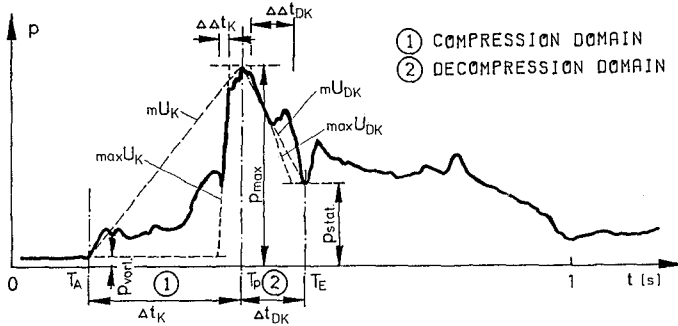


Fig. 1 Definition of anatomy parameters

- the compression domain (Index K) from the beginning up to the peak pressure
- the decompression domain (Index DK) from the peak pressure value to the minimum pressure at the beginning of the quasi-static domain, with the following anatomy parameters:

P_{ws}	[10^4 Pa]	- pressure at begin (thickness of watersheet)
P_{max}	[10^4 Pa]	- maximum (peak) pressure value
P_{stat}	[10^4 Pa]	- min. pressure at begin of quasi-static domain
Δt	[s]	- total times
$\Delta \Delta t$	[s]	- minimum significant times
mU	[10^4 Pa/s]	- mean velocities
$Max U$	[10^4 Pa/s]	- maximum significant velocities

The application of this parameterizing mode is demonstrated in fig. 2 for both domains by an example of an individual shock pressure event, measured in field on a slope 1:4 in vertical steps of 9 cm. In this figure the local distributions of the anatomy parameters, analyzed from the measured pressure-time histories, are plotted versus $\Delta D / H^{1/3}$, which is the vertical distance from stillwaterlevel related to significant waveheight $H^{1/3}$.

From such distributons of single shock pressure events some general remarks may be stated: It is obviuos, that for the higher peak pressures P_{max} the rising times Δt tend to minimum values in the range of about 10 to 50 milliseconds and the corresponding rising velocities to maximum values of about 10 to 1000 m/s. Further higher peak pressures only occur, where the watersheet pressures P_{ws} are low or tends to zero, which demonstrates the wellknown damping effect of a watersheet (FÜHRBÖTER, 1986). Below the range of highest peak pressures on the dyke

COMPRESSION DOMAIN

DECOMPRESSION DOMAIN

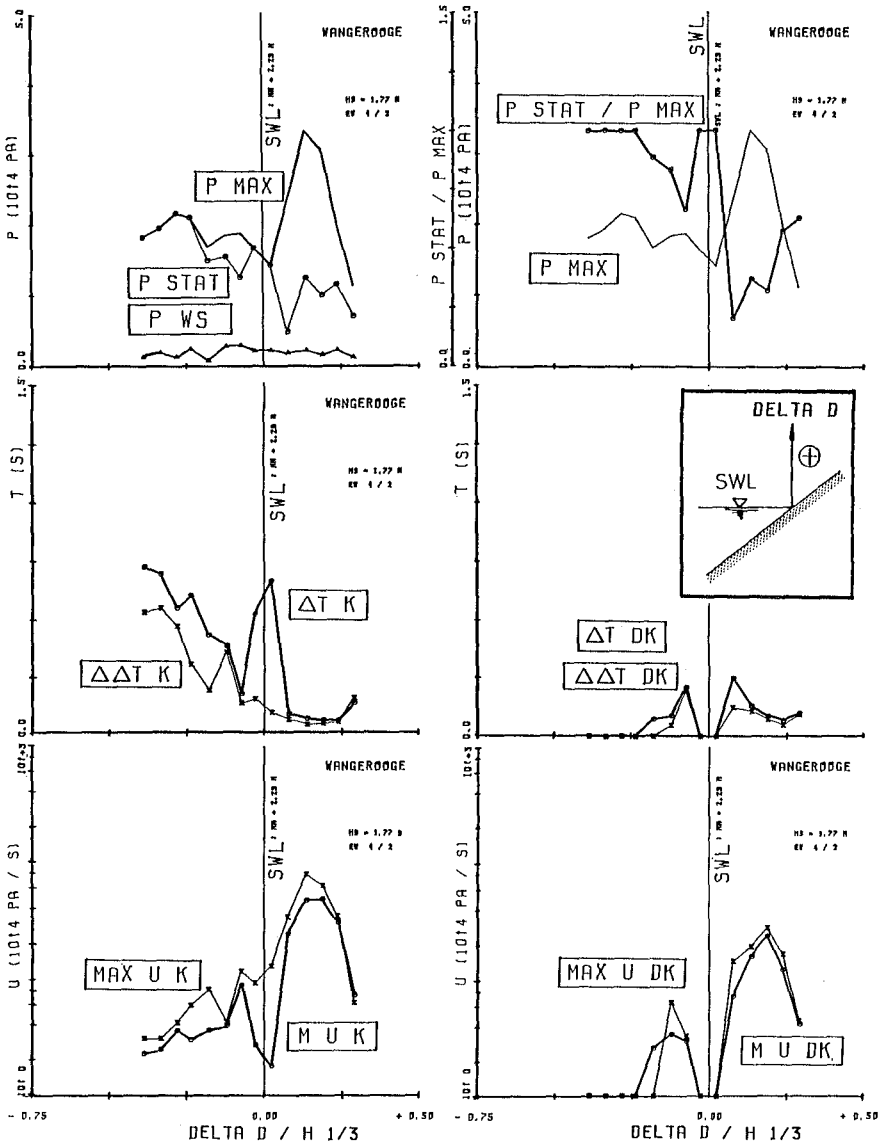


Fig. 2 Local distributions of anatomy parameters

surface, the decompression times and velocities have (tend to) zero values, where the pressures P_{stat} are equal to the (tend to same value as) the P_{max} ones.

It must be mentioned, that the selected example in fig. 2 is a typical one of the classic types and therefore it represents a certain generalisation. Nevertheless, also chaotic types show more or less similar elements, as demonstrated by GRÜNE (1988a). Thus such an analyzing method makes a distinctiveness in relation to real shock pressure occurrence possible.

GENERALISATION OF SHOCK PRESSURE OCCURRENCE

In spite of all the different shock pressure types including the chaotic ones, it was possible to evaluate a generalized model of occurrence with respect to deterministic and stochastic characteristics. The deterministic parts of the model are represented by the local distributions of the anatomy parameters as given in fig. 3 for both domains. The x-axis $\Delta D / H$ in fig. 3 is related to the point on the surface, where $max P_{max}$ occur, instead of the stillwaterlevel in fig. 2. For the stochastic parts stand the superposition with the stochastic fluctuations of the anatomy parameters as shown in the following.

The local distributions in fig. 3 may be divided into five different local ranges, which in figs. 3 and 4 are marked from 1 to 5, each range represents a certain state during the wave breaking process on the slope surface (fig. 4):

- Nr. 1 : This range represents the approaching steep wave front.
- Nr. 2 : At this range the steep wave front has its maximum height, which means the breaker point.
- Nr. 3 : This range gives the area between breaking wave front and the area, where the breaker tongue hits the slope surface. In this range the most chaotic pressure-time histories were found due to the enclosed air pockets with high turbulence.
- Nr. 4 : This is the range, where the breaker tongue hits the surface and thus where real significant shock pressures occur.
- Nr. 5 : This range represents the steep front of wave run-up.

Comparing the distributions of both domains in fig. 3, there are considerable differences for the time parameters. This is mainly due to the fact, that during the wave breaking process the compression times have substantial values except on the local range, where the breaker tongue hits the surface, whereas the decompression times mostly tend to zero values, either because the quasi-static pressures P_{stat} have the same magnitude as P_{max} or because the decompression shapes of the pressure-time histories have the same characteristics as the compression shape. This comes out more clearly by comparing the time distributions with the velocity distributions. Low time values and low velocity values indicate poor or no similarity between compression and decompression characteristic, whereas low times together with high

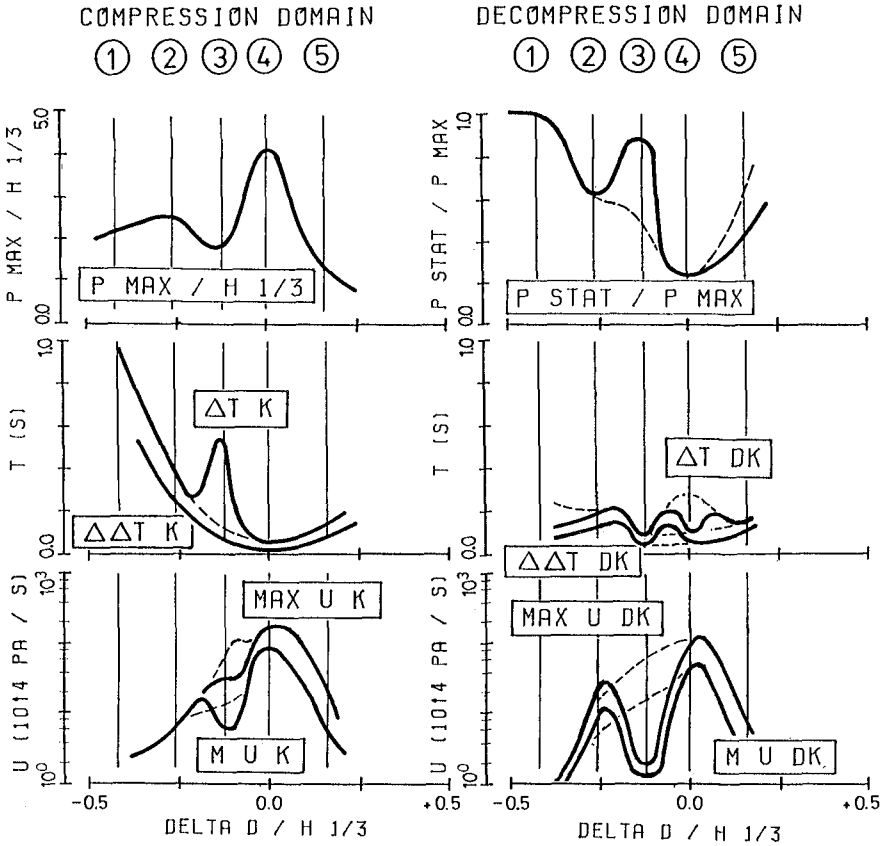


Fig. 3 Local distributions of deterministic parts of anatomy parameters

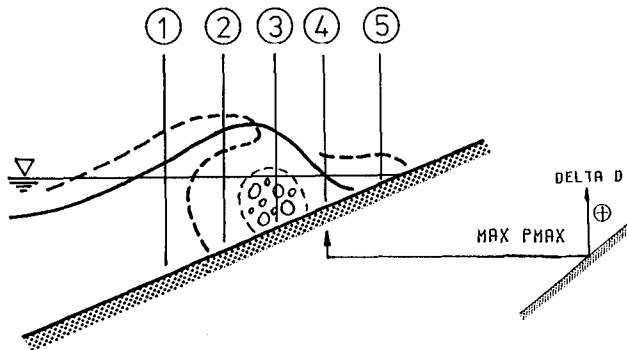


Fig. 4 Scheme of local ranges representing the wave breaking process

velocity values indicate a strong similarity between both domains. Furthermore the model demonstrates, that real shock pressures on slopes only are induced by the breaker tongue hitting on the the surface. Consequently for theoretical considerations the BAGNOLD piston model from the author's physical point of view cannot be used with respect to maximum pressure values on slopes.

RELATIONS BETWEEN ANATOMY PARAMETERS

Due to the occurrence of numberless different shapes of pressure-time histories the data of the different anatomy parameters at a first sight spread like stars at the sky, but nevertheless there are some clear tendencies and some envelope conditions. There are many possibilities of relating the parameters among one another, in this paper all parameters are related to the peak values P_{max} .

In fig. 5 the parameter P_{ws} , which represents the thickness of the watersheet before the shock pressure occurrence, is related to P_{max} . The clear tendency comes out by the envelope curve and also by the density-distribution of the data cloud, that higher peak values P_{max} only occur with decreasing watersheet thicknesses.

Similar tendencies in dependence on higher peak values exist for some more parameters, for example in fig. 6 the time parameters ΔT and $\Delta \Delta T$ of both domains are plotted versus P_{max} . The ratios between both parameters gave no tendency. Differences between ΔT and $\Delta \Delta T$ may be found by the envelope curves and also be seen by the density distribution.

The mean velocities $m U$ of both domains are plotted in fig. 7 versus P_{max} . The data have a wide range of spreading just as the maximum velocity ones. The ratios between the maximum and mean velocities $max U / m U$ of both domains are given in fig. 8. From the density distribution it can be stated, that in most cases the maximum velocities are roughly in the same order of magnitude or only a few times higher than the mean velocities and furthermore, that there is less scatter for the decompression ratios. For higher peak pressures P_{max} the maximum velocity values may be roughly up to five times higher than the mean values.

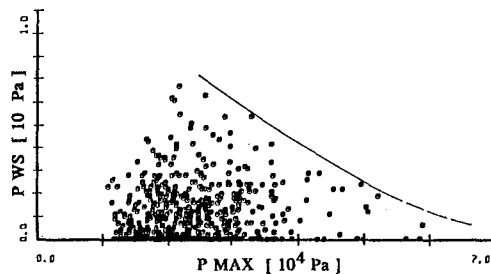


Fig. 5 P_{ws} versus P_{max}

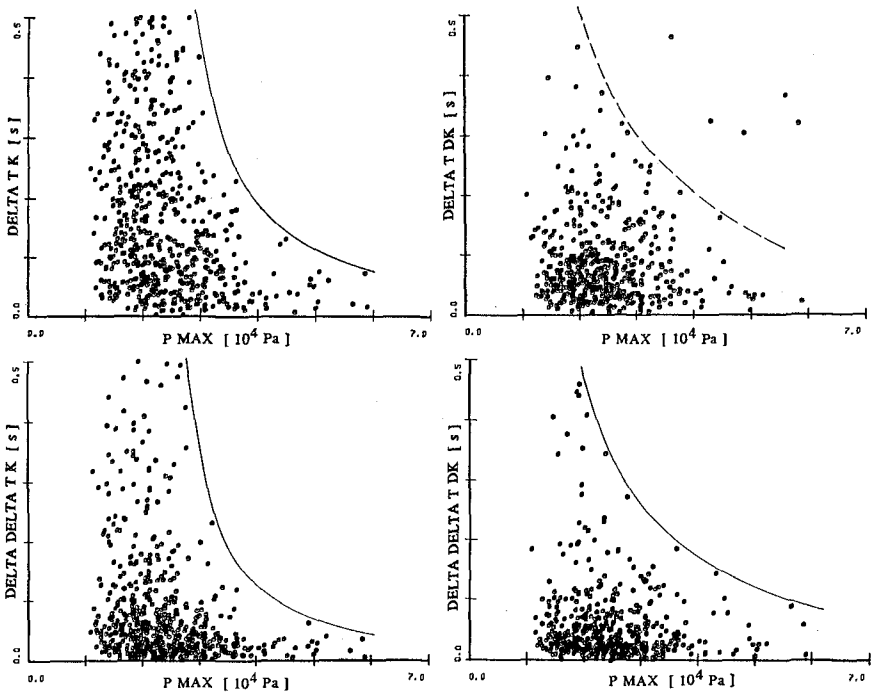


Fig. 6 Total and min. significant compression and decompression times versus P_{max}

Comparisons between compression and decompression parameters are given in figs. 9 and 10. In fig. 9 the ratios for total and minimum significant parameters are plotted versus P_{max} . It is obvious, that in both domains generally the times can be shorter or longer compared to the other domain, but with higher peak pressures P_{max} the compression times decrease relatively more compared to the decompression times and thus the ratios tend to values around 1.0. The comparison of the velocity ratios

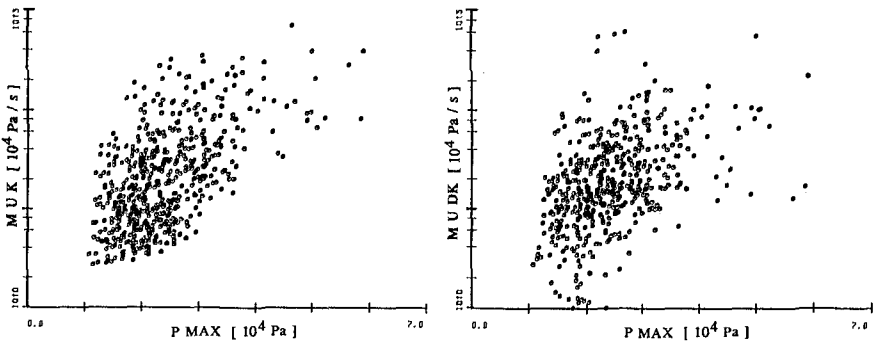


Fig. 7 Mean and maximum compression and decompression velocities versus P_{max}

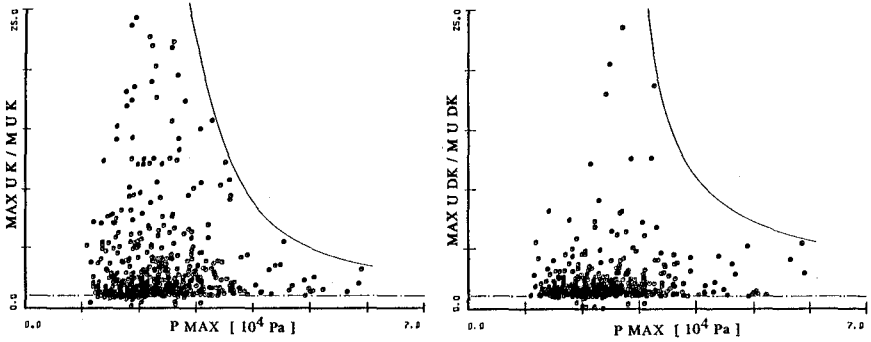


Fig. 8 Ratios between maximum and mean velocities of both domains versus P_{max}

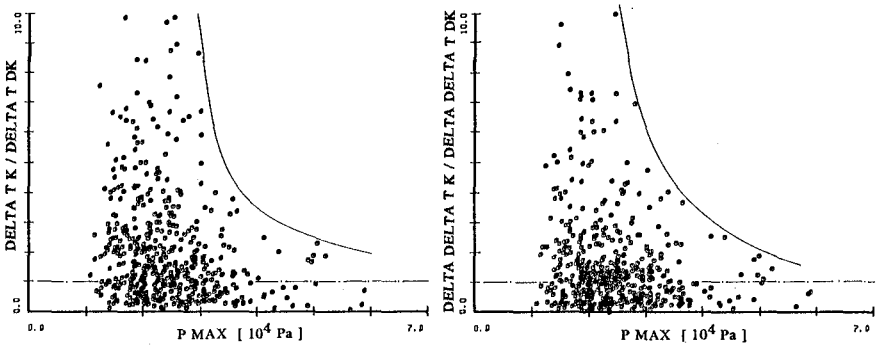


Fig. 9 Comparison between both domains for total and min. significant times

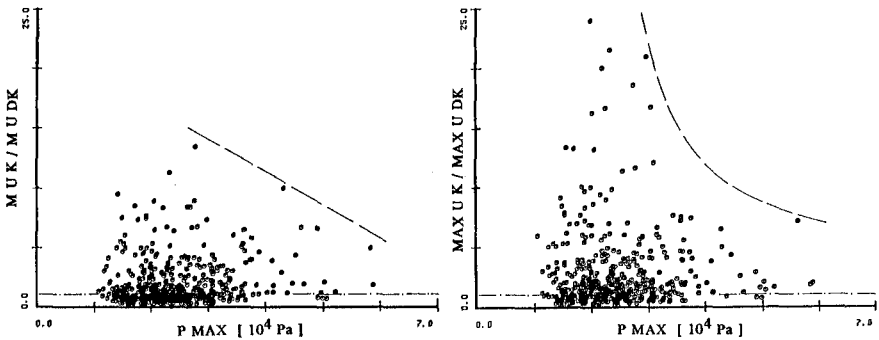


Fig. 10 Comparison between both domains for mean and maximum velocities

in fig. 10 shows more smaller ratio values for mean velocities $m U$. The density-distribution of the data indicate, that in most cases in both domains the velocity values are roughly in the same order of magnitude.

COMPARISON OF PEAK PRESSURES FROM FIELD AND LABORATORY

The peak pressures measured in field were compared with those from large-scale laboratory tests, which have been done in the LARGE WAVE CHANNEL (GWK) of Universities at Hannover and Braunschweig, Germany (GRÜNE, FÜHRBÖTER, 1976). A research program is running since years, which includes investigations on shock pressures and wave run-up on different uniformly and combined sloped dykes. All dyke profiles have a sand core covered with an asphalt concrete layer (same construction as used for field measurements). The same types of shock pressure sensors and data recording systems were installed in the channel as used for the field measurements (GRÜNE, MALEWSKI, 1985). The first tests on slope 1:4 were done mostly with regular waves. The aim was to produce a collectiv of at least 200 single shock pressure events during each test for statistical considerations and to check the spatial width of pressure occurrence (FÜHRBÖTER, 1986).

For comparison of regular wave test data with field data some facts have to be considered:

- firstly one don't know, which wave height should be used. This problem is an old and suffering one, since tests were run in laboratories.
- secondly one have to notice, that regular waves have a more or less constant breaker point and thus the zone, where the breaker tongue hits the slope surface, is a rather narrow one. The thickness of the watersheets from the regular wave run-ups of the preceeding waves also are rather constant, mostly with a certain value (FÜHRBÖTER, 1986). Both conditions are contrary to irregular wave conditions, where the thickness together with the hitting zone of the breakertongue have a broad spreading characteristic. These conditions can be attenuated by the three-dimensionality of real sea state waves and by non oblique wave attack. This may result in higher

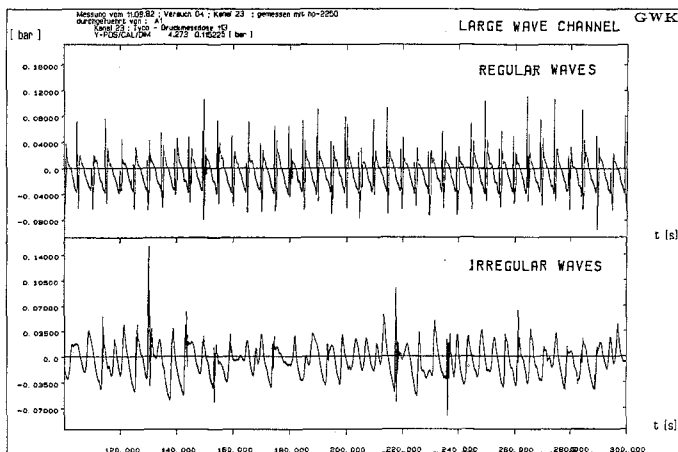


Fig. 11 Pressures on dyke surface induced by regular and irregular waves

shock pressures, if the breaker tongue of a high wave hits the slope surface at such a moment, when the watersheet is zero or tends to zero. Furthermore, as demonstrated in fig. 11 for the same pressure sensor and roughly the same waveheights, each regular wave gives a peak pressure value, which cannot be found for irregular waves. This leads to different statistical characteristics of the data (GRÜNE, 1988b).

In fig. 12 the statistical peak pressure values $P_{99.9}$ from field and from GWK-tests with regular waves (FÜHRBÖTER, 1986) have been compared. Each value was derived from log-normal distributions of all peak pressures measured during one time interval on a slope 1:4 with all installed sensors. Both the data from field and laboratory are related to mean wave heights H_m . For all data the agreement is rather poor, but it must be mentioned, that there are also differences between the field data, due to different wave climate characteristics at the two locations. The wave characteristics of the laboratory tests were similar to those at Eiderdamm location. It is obvious,

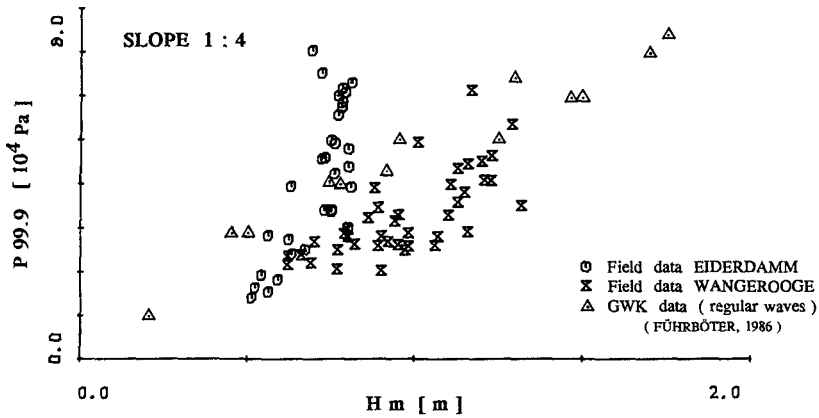


Fig. 12 Comparison between field and large scale test data with regular waves

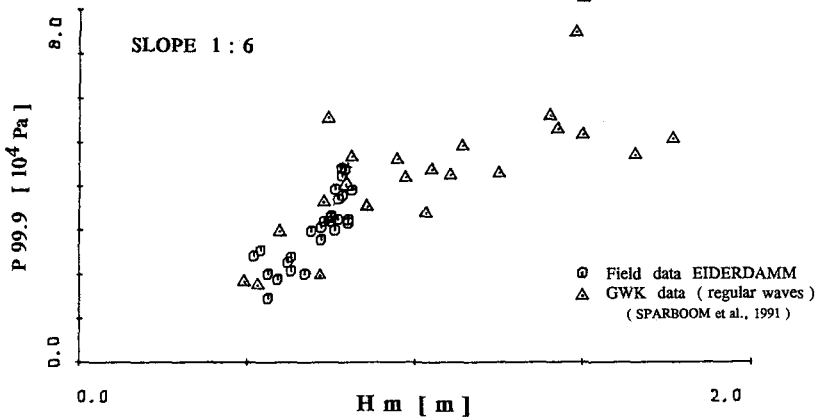


Fig. 13 Comparison between field and large scale test data with regular waves

that higher field pressure values were found. Further comparisons have shown, that even, if one relate the field data to significant waveheight $H/3$, there are some few higher pressure data. A comparison of field data for the slope 1 : 6 with GWK data (SPARBOOM et al., 1991) in fig. 13 shows a fairly well agreement. The differences of the GWK data between both slopes are rather small compared with those, found for field data (GRÜNE, 1988b).

Fig. 14 shows a comparison with a few GWK data, measured with irregular waves on slope 1:6. The data are as well related to mean waveheights H_m as to waveheights $H/3$. The agreement is much better compared to data measured with regular waves, nevertheless the laboratory data give the impression of a tendency to higher pressure values. If one use the actual measured maximum peak pressure values $max P_{max}$ of each measured time interval or test, instead of the statistical values

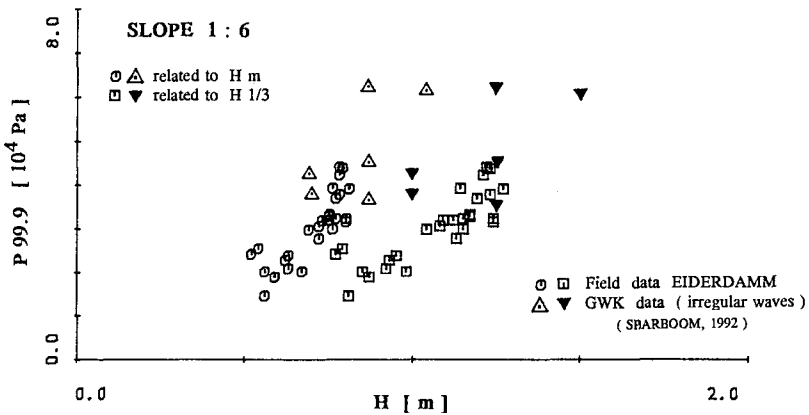


Fig.14 Comparison between field and large scale test data with irregular waves

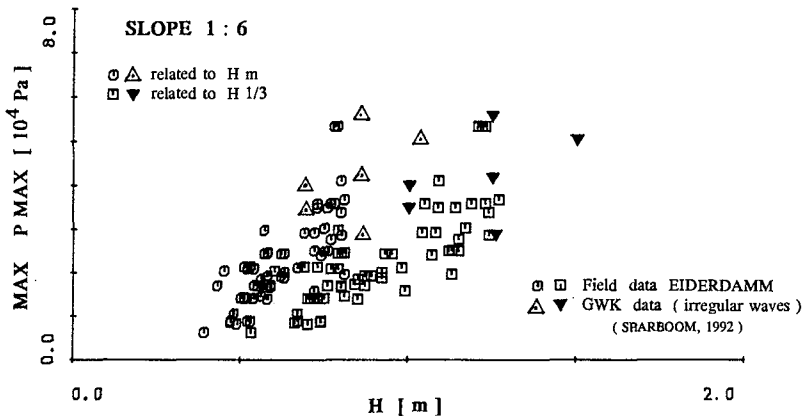


Fig. 15 Comparison between field and large scale test data with irregular waves

P 99.9, then the agreement between field and laboratory is quite well for these data as shown in fig. 15. Further comparisons have shown a quite well agreement with field data even for laboratory data from regular wave tests by using the *max Pmax* parameter related to *Hm*. From this results one may state, that comparison between field and laboratory data from regular waves tests both should be related to mean waveheight *Hm*, which is also the cleanest way from the definition point of view.

A " DYNAMIC " LOADING MODEL

A first approximation for a loading model has based on the local peak pressure parameter distributions, found for individual breaking wave events (GRÜNE, 1988b). Although the several values of these distributions have small phase lags mutually, they may give a realistic approximation of a worst-case loading model. The next developing step was, to evaluate actual synchronous pressure distributions without any phase lag from the recorded pressure-time histories.

On the lefthand in fig. 16 the pressure-time histories of one individual shock pressure event, measured with the sensors D8 to D21 in local steps on the surface, are plotted. The horizontal time axis is divided in 12 steps and for each time step the

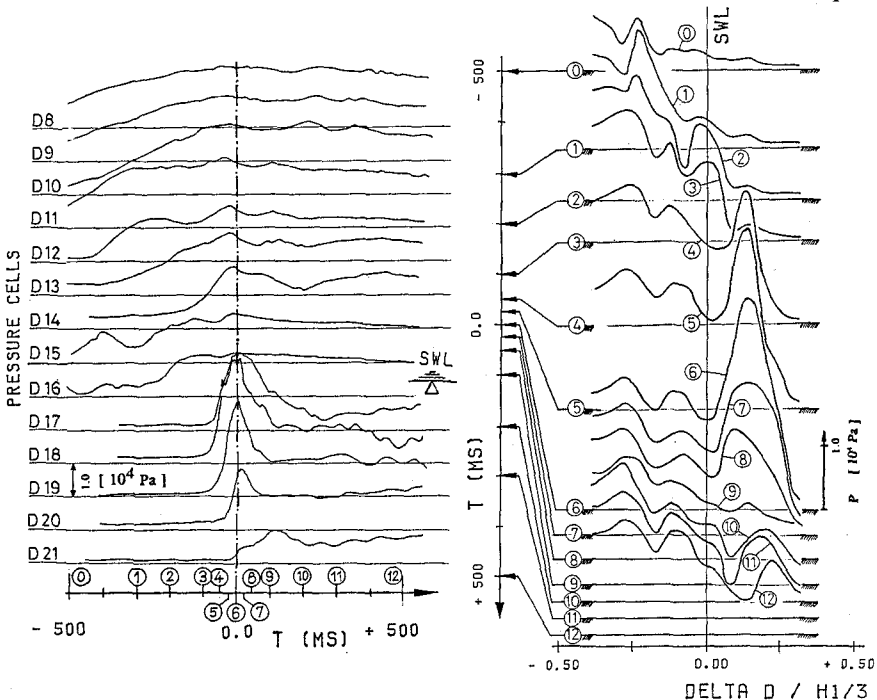


Fig. 16 Measured pressure-time histories (lefthand part) and evaluated actual pressure distributions (righthand part) for one individual breaking wave

pressure values at the certain levels were used to evaluate actual pressure distributions on the surface as plotted in the righthand part of fig. 16. There the time axis is the vertical axis, whereas the horizontal axis represents the slope surface, defined as the vertical distance from stillwaterlevel *SWL* related to $H/3$. From comparisons between the evaluated maximum actual pressure distributions and the local peak pressure distributions from the pressure-time histories it was found, that the actual distributions mostly are a bit narrower.

Based on such actual pressure distributions, a new version of the loading model was created, which is given in fig. 17. Compared with the first version the shape was modified with respect to linear geometrical pressure boundaries for simpler application. Each of these geometrical boundary conditions (marked with a circled number in fig. 17), which are derived from the anatomy parameter results, have to be varied systematically within certain ranges (listed in Table 1), to find out the

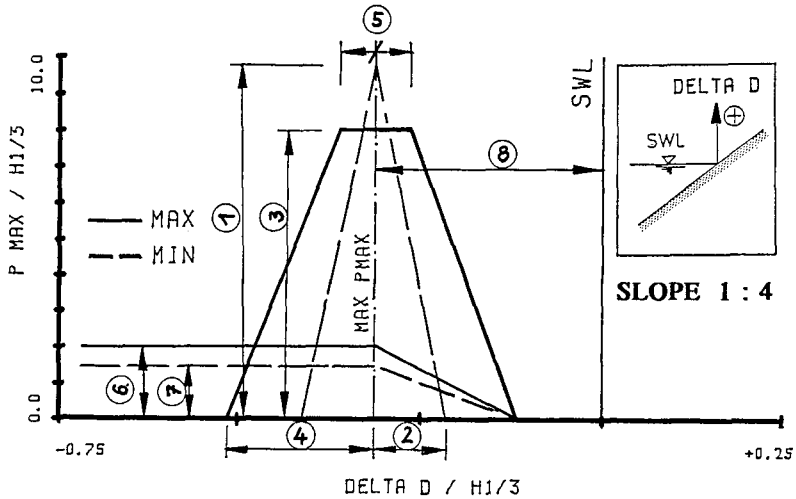


Fig. 17 "Dynamic" loading model for slope 1 : 4

			RANGE	
S	①	peakpressure	$3.0 \leq P_{max} / H1/3 \leq 10.0$	MIN
S	②	acting width	$0.10 \leq \Delta D / H1/3 \leq 0.25$	MIN
S	③	peakpressure	$3.0 \leq P_{max} / H1/3 \leq 8.0$	MAX
S	④	acting width	$0.15 \leq \Delta D / H1/3 \leq 0.30$	MAX
S	⑤	acting width	$0.05 \leq \Delta D / H1/3 \leq 0.10$	MAX
W	⑥	wavepressure	$P_{max} / H 1/3 \leq 2.0$	MAX
W	⑦	wavepressure	$P_{max} / H 1/3 \leq 1.5$	MIN
S	⑧	acting point	$-1.0 \leq \Delta D / H 1/3 \leq +0.5$	

Table 1 Ranges for boundary conditions of the loading model in fig. 17

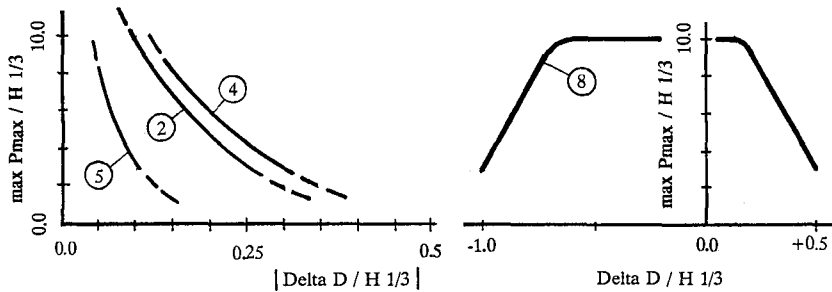


Fig. 18 Boundary conditions in dependence of $\max P_{\max} / H^{1/3}$

worst case load. Fig. 18 shows the relations between the $\max P_{\max} / H^{1/3}$ values and the different acting widths $|\Delta D / H^{1/3}|$ (lefthand part) and the acting center line of the loading model related to the vertical distance $\Delta D / H^{1/3}$ from stillwaterlevel *SWL* (righthand part). It must be mentioned, that the boundary conditions represent the worst case actual pressure distributions and thus most of recorded shock pressure events have smaller ones.

ACKNOWLEDGEMENTS

The research work partly was done by the SONDERFORSCHUNGSBEREICH 205 / A 1 (supervision Prof. Dr.-Ing. Führbötter) and has been supported by the GERMAN RESEARCH FOUNDATION (DFG).

REFERENCES

- FÜHRBÖTER, A. (1986). Model and prototype tests for wave impact and run-up on a uniform 1:4 slope. *Coastal Engineering*, 10, pp. 49-84.
- GRÜNE, J., FÜHRBÖTER, A. (1976). Large wave channel for "full-scale modeling" of wave dynamics in surf zones. *Proc. of Symp. on Modeling Techniques, San Francisco*, pp. 82-100.
- GRÜNE, J., MALEWSKI, W. (1985). Design and construction of a GWK 1:4 test slope for investigations on shock pressures and run-ups. *Technical report SFB 205/A1 (in german)*, unpublished.
- GRÜNE, J. (1988a). Anatomy of shock pressures (surface and sand core) induced by real sea state breaking waves. *Proc. of the Intern. Symp. on Modelling Soil-Water-Structure Interactions (SOWAS 88), Delft*, pp. 261-270.
- GRÜNE, J. (1988b). Wave-induced shock pressures under real sea state conditions. *Proc. of the 21st International Conference on Coastal Engineering (ICCE '88), Malaga*, pp. 2340-2354.
- SPARBOOM, U., DEBUS, W. (1991). Local shock pressure distribution on a 1:6 slope in GWK (regular waves). *Technical report SFB 205/A1 (in german)*, unpublished.
- SPARBOOM, U. (1992). Personal communication, manuscript for a *Techn. Report*.